

Synthesis of CuMoO₄ Nanostructures Using Tridax Procumbens Leaf Extract: Enhanced Crystal Violet (CV) as Anionic Dye Degradation

M. Aswin, Ambrose Rejo Jeice*

Department of Physics & Research Centre, Annai Velankanni College, Tholayavattam, 629157, Tamil Nadu, India, Affiliated to Manonmaniam Sundaranar University, Abishekapatti, Tirunelveli, 627012, Tamil Nadu, India

ABSTRACT: Tridax procumbens leaf extract (T.procumbens) is utilized to synthesize Cupric molybdate nanostructures (CuMoO₄), which are environmentally safe and can be employed as capping or reducing agents. Using UV-vis spectroscopy, XRD, SEM, and EDS, the optical, structural, and morphological properties of CuMoO₄ are investigated. SEM and EDS confirmed the nanorod shape and purity of CuMoO₄ nanostructures. UV-vis spectroscopy, which demonstrated surface plasmonic resonance at 300–500 nm, confirmed the synthesis, while XRD revealed the produced nanostructures to be in a triclinic or anorthic phase. The synthesized CuMoO₄ nanostructures demonstrated a >90% degradation efficiency when exposed to solar irradiation and were used as a photocatalyst for the filtration of water contaminated with crystal violet (CV) dye. As a result, this study presents a promising, simple, affordable, and environmentally friendly biosynthesis of CuMoO₄ photocatalyst that may be used to clean up dye-polluted water.

KEYWORDS: Green synthesis; CuMoO₄ nanostructures; photocatalytic activity; Tridax procumbens

<https://doi.org/10.29294/IJASE.10.3.2024.3489-3494> ©2024 Mahendrapublications.com, All rights reserved

1.0 INTRODUCTION

Researchers are looking for environmentally friendly and less hazardous ways to produce and apply nanomaterials, which can reduce health risks, prevent waste from forming or building up, and create reusable and biodegradable products using renewable raw materials in response to the alarming environmental issues of our day. Green synthesis, a subfield of emerging green nanotechnology, aids in the environmentally friendly synthesis of nanomaterials without the use of hazardous chemicals, and it has the potential to be a useful approach to solving all of these issues [1,2]. Nanomaterials have been effective in eliminating dye pollutants by photocatalytic activities in recent years, despite their many forms, shapes, and sizes. The reason for this is their distinct physicochemical characteristics, which include their high surface area, a modest advantage in metal/semi-metallic weight and behaviour, high thermal and electrical conductivities, high mechanical strength, and high width-to-height ratio. Copper, zinc, molybdenum, and titanium are

just a few of the nanomaterials that are used in the treatment of textile waste dyes and other dye treatments such as photo-degradation, adsorption, precipitation, and decolorization. Since synthetic dyes are very poisonous, have a low biological degradability, are harmful to a wide range of creatures, and are harmful to human health, their discharge in the aquatic environment as wastewater from the textile sector raises ecological concerns [3,4]. A little over 15% of these heavy, hazardous synthetic textile dyes are released into aquatic bodies untreated each year through textile wastewater. Numerous techniques, including coagulation, microbial degradation, active sludge, reverse osmosis, and ultra-filtration, have been employed in recent years for the management of wastewater. Unfortunately, due to their chemical stability, most synthetic dyes remain in water even after being treated with dye effluent. According to recent studies, the most effective and widely applied technique for getting rid of synthetic dyes is photocatalytic degradation, which uses metal semiconductors

*Corresponding Author: rejojeice@gmail.com

Received: 11.01.2024

Accepted: 17.02.2024

Published on: 07.03.2024

Aswin & Ambrose Rejo Jeice

such as NiO, TiO₂, ZnO, CeO₂, MoO₃, and CuO [5]. CuMoO₄ is one of the semiconductor nanoparticles with the most distinctive properties; its low cost, non-toxicity, and photostability make it an efficient photocatalyst for the deterioration of textile colors. The cost-effective biosynthesis of CuMoO₄ nanostructures was examined in this research work, which used *T.procumbens* plant leaf extract as a natural reducing and stabilizing agent. The *T.procumbens* plant contains a high concentration of phyto compounds that improve the biological qualities of CuMoO₄ nanostructures while also lowering their toxicity. The produced CuMoO₄ nanostructures were utilized as photocatalysts against industrial dye in aqueous solution.

2. EXPERIMENTAL SECTION

2.1. Materials used

All analytical grade (AR) chemicals were utilized here. Copper (II) chloride dihydrate (CuCl₂·2H₂O) from LOBA Chemie, India, Ammonium heptamolybdate tetrahydrate (AHM) (NH₄)₆Mo₇O₂₄·4H₂O from LOBA Chemie, India, Whatman filter paper (Grade No.1), *T.procumbens* leaves (collected from local area in Kanyakumari, India), deionized water was used throughout the synthesis process.

2.2. Preparation of *T.procumbens* leaf extract

After collection, the leaves were washed with distilled water for the removal of impurities residing on the surface of the leaves. Then the purified leaves cut into smaller pieces, and after this, 20g of the cut part was subjected in 100 ml of distilled water and allowed to stir for 1h at 70°C. the obtained extract was ultimately filtered through Whatman No.1 filter paper and kept in a covered conical flask for further usage.

2.3. Synthesis process

Green mediated hydrothermal method employed in this synthesis process of CuMoO₄ nanostructures. 100 ml of 0.1 M AHM was taken in a 250 ml beaker and stirred vigorously for 60 minutes at 70°C and 10 ml of the newly manufactured leaf extract was mixed dropwise under constant stirring. 100 ml of 0.05M CuCl₂·2H₂O stirred for 60 minutes. After 30 minutes, stirred solution of CuCl₂·2H₂O mixed dropwise into them and finally, after 60 minutes the residues forms indicated the formation of CuMoO₄ nanostructures. The solution obtained was then washed and centrifuged various times

with distilled water and filtered via Whatman No.1 filter paper. The filtered sample was dried in hot air oven at 120 °C for 8h. The dried sample was transferred into the silica crucible was placed at muffle furnace then heated 530 °C for an hour.

2.4. Characterization techniques

Crystallinity of CuMoO₄ at 2θ degrees between 10-60° was examined using XRD (Bruker D8 Advance Diffractometer using CuKα1 radiation (1.540 Å) at 30 kV and 40 mA). The typical absorption peak of CuMoO₄ nanostructures at a wavelength range of 200-800 nm was observed using a UV-Vis-Lambda 650 Spectrophotometer (Perkin Elmer). The morphology and elemental composition were examined using SEM-EDS (KYKY-EM3200, 25 kV) system.

3. RESULTS AND DISCUSSION

3.1. Structural and Phase analysis

Fig. 1 displays the XRD pattern that was used to precisely identify the produced CuMoO₄ nanostructures. Sharp peaks located at 15.301°, 18.941°, 21.12°, 23.128°, 26.181°, 32.472° and 37.617° on the CuMoO₄ characteristic intensity spectrum are indexed to the diffraction plans ($\bar{1}$ 0 1), ($\bar{1}$ $\bar{1}$ 1), ($\bar{1}$ 0 2), (0 2 0), ($\bar{1}$ 2 0), (0 $\bar{2}$ 3) and (1 $\bar{2}$ 3) respectively. The intensity peak positions are exactly matched to the triclinic or anorthic structure (JCPDS File No. 89-0228) with lattice parameters of a = 6.306 Å, b = 7.978 Å, and c = 9.710 Å. The average crystalline size of crystal structured of CuMoO₄ nanostructures is 57 nm by using Debye-Scherrer formula is $D = \frac{k\lambda}{\beta \cos \theta}$, where λ is the wavelength used (i.e., 1.54 Å), k is Scherrer constant, θ is the Bragg's angle of diffraction and β is the full width half maxima [6].

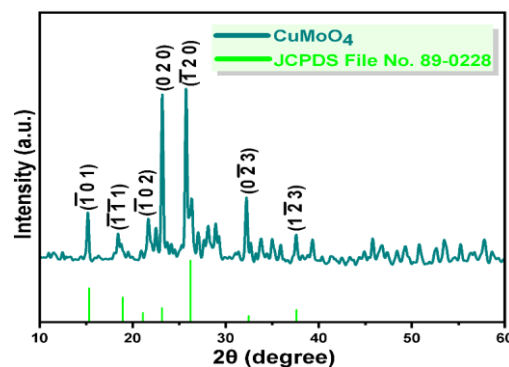


Fig.1.XRD patterns of CuMoO₄ nanostructures

3.2. Band gap determination from optical studies

Figure 2(a) displays the UV-vis absorbance spectra of green produced CuMoO_4 nanostructures in the UV-vis range. UV-vis absorption spectra, in the wavelength range between 200 and 800 nm. We can use the following formula to find the absorption band gap E_g , $\alpha h\nu = (h\nu - E_g)^n$, in which n is either $1/2$ for an indirect transition or 2 for a direct transition, $h\nu$ is the photoenergy, α is the

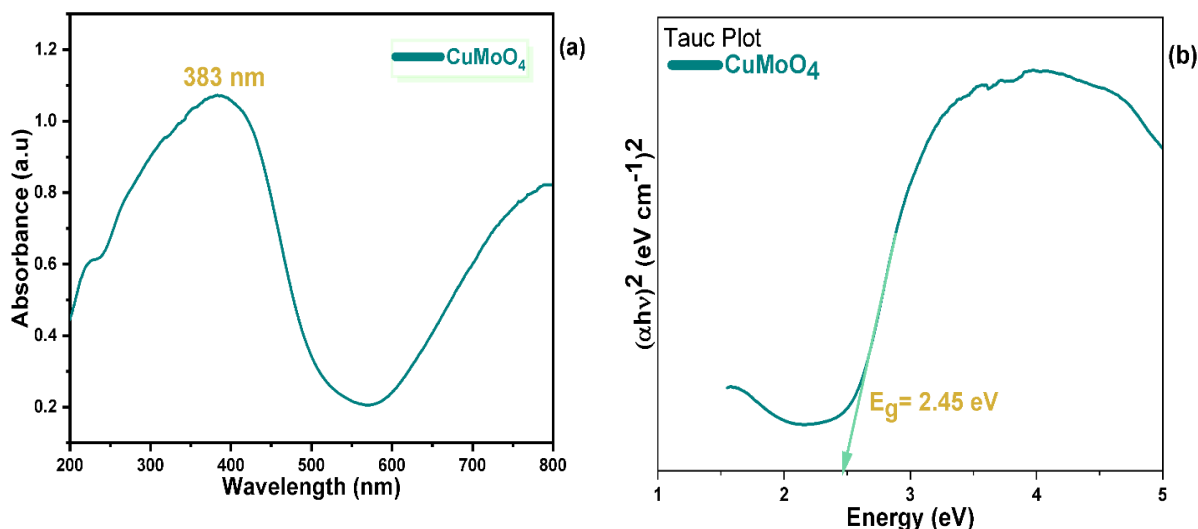


Fig.2. (a) UV-vis spectra, (b) Direct bandgap energy showed Tauc plot of CuMoO_4 nanostructures

3.3. Scanning Electron Microscope (SEM) with Energy Dispersive Spectroscopy (EDS)

Fig. 3 presents SEM and EDS image of the CuMoO_4 nanostructures and illustrates morphological and elemental configuration. The atomic weight percentage of each element in the sample as well as its constituent elements is confirmed by the EDS spectrum. Fig. 3(b) shows the recorded EDS spectrum of the produced CuMoO_4 nanostructures, which clearly indicates

the presence of Cu and Mo atoms in addition to O. The SEM picture of CuMoO_4 nanostructures, which only has rod like morphology, is displayed in Figure 3a. Furthermore, the type of plant material used and the experimental setup affect the shape and physio-chemical characteristics of nanostructures [8]. The EDS analysis of biosynthesized CuMoO_4 nanostructures indicates that the sample exclusively contains the specified elements Cu, Mo and O, along with their atomic and weight percentages, as shown in the Table.1.

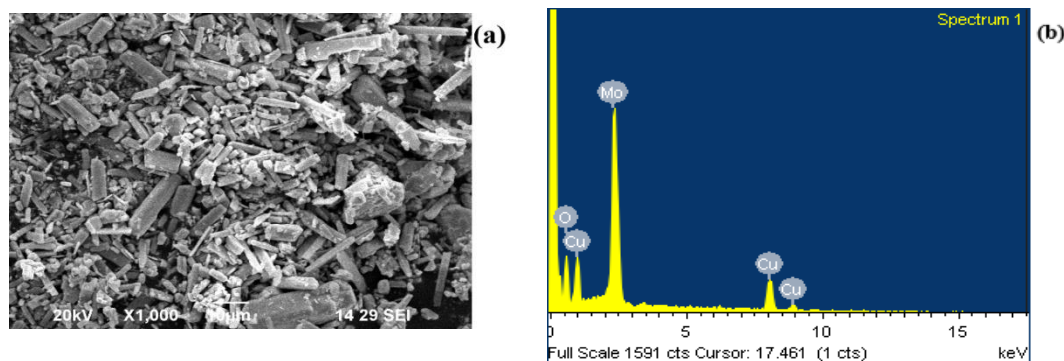
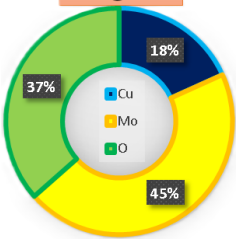
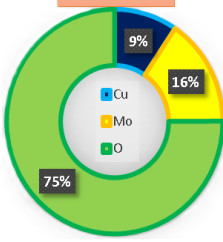


Fig.3 (a,b) SEM image with EDS spectra of CuMoO_4 nanostructure

Table.1. Elemental composition of EDS spectra of CuMoO₄ nanostructure

Sample	Elements	Weight %		Atomic %	
CuMoO ₄	O K	36.52		75.06	
	Cu K	18.24		9.44	
	Mo L	45.24		15.51	

3.4. Photocatalytic Activity

Under solar radiation, photodegradation anionic dye such as crystal violet (CV) 60 ppm in aqueous solutions were used to study the photocatalytic activities of CuMoO₄ nanostructures as catalyst. The UV-vis absorbance intensity maxima and linear plot of CV, which were measured at 550-600 nm for varying time intervals while CuMoO₄ nanostructures were present under solar radiation, are displayed in Figures.4(a,b) respectively. The degradation percentage was determined in each degradation investigations employing equation,

$$\text{Dye degradation (\%)} = \left(1 - \frac{C}{C_0}\right) \times 100$$

Where the absorbance at zero and the absorbance at any time 't' were represented by the values C₀ and C respectively. The efficiency of degradation was compared with control dye solutions in the current study of CuMoO₄ nanostructures in aqueous dye solutions, which lowered intensity of the relative degraded peaks with increase solar irradiation time. After 120 minutes of sun exposure, the greatest percentage of CV degradation was seen 96.96%. The photo-degradation kinetics of the catalysed process was explained using the Longmuir-Hinshelwood model.

$$\ln\left(\frac{C}{C_0}\right) = \ln(A_t/A_0) = -K_{app}t$$

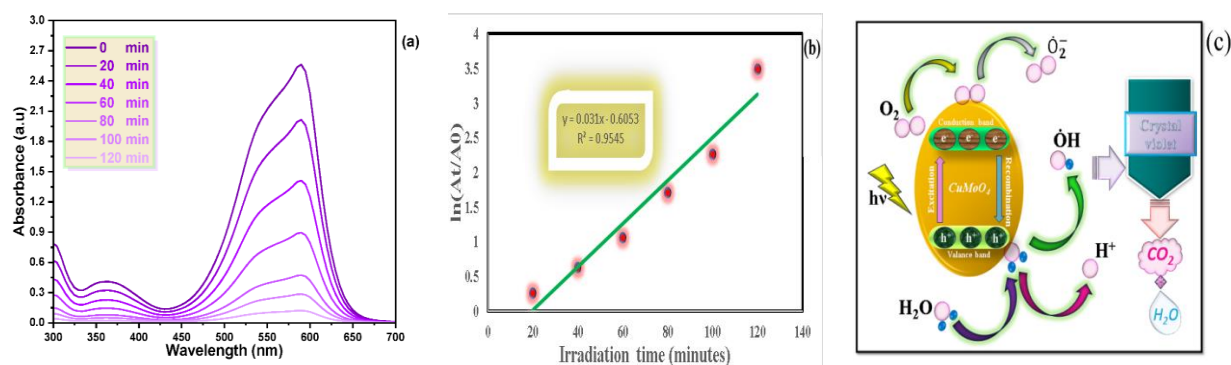


Fig.4(a) Decrease in intensity, (b) linear plot and (c) mechanism of dye degradation of CuMoO₄ nanostructures.

The apparent pseudo-first-order constant (min⁻¹) is represented by (K_{app}), which is the basic form of the model for the apparent pseudo-first-order. A linear function with a slope equal to (K_{app}) represents the plot of ln(C/C₀) against time. When adding produced CuMoO₄ nanostructures to a reaction mixture under solar radiation, the photodegradation of the dye

plays a significant role in the production of active species. When sunlight strikes the surface of CuMoO₄ nanostructures, electrons travel from the VB gap to the CB, creating electron-hole pairs. This is how the catalyst was made. The effectiveness of photocatalytic degradation has improved electron transmission from semiconductors and recombination on the

surface of CuMoO_4 nanostructures. When electron hole pairs react with electron contributors (H_2O and hydroxyl ions), the hydroxyl radical ($\text{OH}\cdot$) is created. During the multi-electron reduction reaction, superoxide radicals are produced when one electron is trapped with oxygen molecules. These radicals then undergo modification to become hydroxyl

radicals. Ultimately, H_2O , CO_2 , and broken-down mineral compounds were generated when active species reacted with aqueous dye molecules [9,10]. Mechanism of dye degradation of CuMoO_4 nanostructure is shown in Figure.4(c). A comparison is made in Table 2 of photocatalytic dye degradation with metal oxide nanostructures.

Table.2 Photocatalytic dye degradation – a comparison with metal oxide nanomaterials.

Nanocatalysts	Synthesis method /Leaf	Dye	Efficiency (%)	Source of light	Irradiation time(min)	Reference
CdO	Veldt Grape	CV	87	UV-vis	120	[11]
CuO	Tridax procumbens	BG	91.09	UV-vis	120	[12]
$\alpha\text{-MoO}_3$	Rhinacanthus nasutus	MB	93.7	UV-vis	120	[13]
Mn_3O_4	Cissus quadrangularis	MB	81	UV-vis	120	[14]
TiO_2	Averrhoa carambola	BG	91	UV-vis	150	[15]
$(\text{CdO})(\text{Mn}_3\text{O}_4)$	Microwave	MB	92	UV-vis	120	[16]
CuMoO_4	Tridax procumbens	CV	96.96	Sun light	120	Present Work

4. CONCLUSION

Tridax procumbens (*T.procumbens*) leaf extract played a crucial role in green synthesis of triclinic or anorthic structured CuMoO_4 nanostructures encapsulated nanorod like morphology. The major phytochemicals, such as phenolic acids, flavonoids, and vitamins are present in the *T.procumbens* leaf extract were believed to play decisive roles of both reducing and capping agents. The characteristics of the green generated CuMoO_4 nanostructures were assessed using analytical techniques such as XRD, UV-vis spectra and SEM-EDS. Photocatalytic studies on CV of CuMoO_4 nanostructures show that dyes can be effectively removed to 96.96% of the time of irradiation.

Acknowledgement

M. Aswin, a research scholar (Reg. No.20213012131015), would like to thank the Department of Physics and Research Centre of Annai Velankanni College, Tholayavattam, for providing the AU 2603 UV-vis double beam spectrophotometer, hot air oven, and muffle furnace.

REFERENCES

- [1] Smith, G.B, Granqvist, C.G. Green Nanotechnology, Taylor and Francis Group, LLC USA, 2011, pp. 1–21
- [2] Ghosh, D., Bhattacharyya, K.G. 2002. Adsorption of Methylene Blue on Kaolinite. Applied Clay Science Appl. Clay Sci. 20 (6) 295–300.
- [3] Sharma, S., Kumar, K., Thakur, Chauhan, NS., Chauhan, M. 2020. The effect of shape and size of ZnO nanoparticles on their antimicrobial and photocatalytic activities: a green approach, Bull. Mater. Sci. 43, 20.
- [4] Singh, J., Dutta T., Kim K.-H., Rawat, M., Samddar, P., Kumar, P. 2018. Green synthesis of metals and their oxide nanoparticles: applications for environmental remediation, J. Nanobiotechnol. 16, 84.
- [5] Salem, S.S., Fouda, A.2020. Green synthesis of metallic nanoparticles and their prospective biotechnological applications: an overview, Biol Trace Elem Res, Jan;199(1):344-370.
- [6] Gawade, V., Gavade N., Shinde, H., Babar, S., Kadam, A., Garadkar, K. 2017. Green

- synthesis of ZnO nanoparticles by using Calotropis procera leaves for the photodegradation of methyl orange, J. Mater. Sci. Mater. Electron. 28,14033–14039.
- [7] He, Y., Zhang, L., Wang, X., Wu, Y., Lin, H., Zhao, L., Weng W., Wan, H., Fan, M. 2014. Enhanced photodegradation activity of methyl orange over Z-scheme type MoO₃-g-C₃N₄ composite under visible light irradiation, RSC Adv. 4(26) 13610–13619.
- [8] Madhusudan, P., Jingrun, R., Zhang, J., Yu, J., Liu, G. 2011. Novel urea assisted hydrothermal synthesis of hierarchical BiVO₄/Bi₂O₂CO₃ nanocomposites with enhanced visible-light photocatalytic activity, Appl. Catal. B Environ. 110, 286–295.
- [9] Li, W., Zhao, S., Qi, B., Du, Y., Wang, X., Huo, M. 2010. Appl. Catal. B Environ. 92 (3) (2009) 333–340.
- [10] S. Zhao, J. Li, L. Wang, X. Wang, Clean Soil Air Water 38 (3) (2010) 268–274.
- [11] Rajaram, P., Samson Y., Jeice, A. R. 2023. Synthesis of Cd(OH)₂-CdO Nanoparticles using Veldt Grape Leaf Extract: Enhanced Dye Degradation and Microbial Resistance, BioNanoScience, 13, 1289–1307.
- [12] Aswin, M., Ambrose Rejo Jeice. 2023. Photocatalytic activity of green fabricated CuO bionanoparticles using Tridax procumbens leaves extracted in divergent medium with antimicrobial facets. Biomass Conv. Bioref. 1-17.
- [13] Aswin Manikanda Vasan, Ambrose Rejo Jeice, Prammitha Rajaram, 2023. Photocatalytic investigations of biogenic α -MoO₃ nanorods influences of the leaves extracted in a divergent medium of Rhinacanthus nasutus against triple count of cationic dyes and antimicrobial activity. Journal of Molecular Structure, Feb. 137800 (In Press).
- [14] Rajaram, P., Jeice, A.R., Jayakumar, K. (2023). Green synthesis of orthorhombic Mn₂O₃ nanoparticles; influence of the oxygen vacancies on antimicrobial activity and cationic dye degradation. New Journal of Chemistry, 47(38) 17734-17745.
- [15] Prammitha, R., Jeice, A.R., Jayakumar, K. 2023. Influences of calcination temperature on titanium dioxide nanoparticles synthesized using Averrhoa carambola leaf extract: in vitro antimicrobial activity and UV-light catalyzed degradation of textile wastewater, Biomass Conversion and Biorefinery, 14, 1-14.
- [16] Jebisha, S., Deepa G., Johnson, J. Mahadevan, C.K. 2024. Synthesis, properties and applications of sulfur doped (CdO)_{1-x} (Mn₃O₄)_x (X=0.0/0.25/0.50/0.75/1.0) nanocrystals. Materials Chemistry and Physics, 314, 128897.